International Journal of Architectural, Civil and Construction Sciences
ISSN: 2415-1734
Vol:13, No:2, 2019

Investigation of Seismic T-Resisting Frame with Shear and Flexural Yield of Horizontal Plate Girders

Helia Barzegar Sedigh, Farzaneh Hamedi, Payam Ashtari

***Abstract*—**There are some limitations in common structural systems, such as providing appropriate lateral stiffness, adequate ductility, and architectural openings at the same time. Consequently, the concept of T-Resisting Frame (TRF) has been introduced to overcome all these deficiencies. The configuration of TRF in this study is a Vertical Plate Girder (VPG) which is placed within the span and two Horizontal Plate Girders (HPGs) connect VPG to side columns at each story level by the use of rigid connections. System performance is improved by utilizing rigid connections in side columns base joint. Shear yield of HPGs causes energy dissipation in TRF; therefore, high plastic deformation in web of HPGs and VPG affects the ductility of system. Moreover, in order to prevent shear buckling in web of TRF's members and appropriate criteria for placement of web stiffeners are applied. In this paper, an experimental study is conducted by applying cyclic loading and using finite element models and numerical studies such as push over method are assessed on shear and flexural yielding of HPGs. As a result, seismic parameters indicate adequate lateral stiffness, and high ductility factor of 6.73, and HPGs' shear yielding achieved as a proof of TRF's better performance.

***Keywords*—**Experimental study, finite element model, flexural and shear yielding, T-resisting frame.

I. Introduction

INTRODUCING new earthquake resistant systems with adequate energy dissipation is essential to prevent structural failure under severe earthquakes by emphasizing providing sufficient ductility, strength, and lateral stiffness. Since an increase in stiffness results in a decrease in ductility, it is desirable to devise a structural system which provides these properties in an optimum level without excessive costs.

TRF consists of VPG with high depth of web, which is located at the middle of span and jointed to side columns by two HPGs. Using the entire capacity of HPGs' web with respect to shear yielding, rigid connections of link beams (HPGs), and even rigid base connection of TRF's vertical members may improve the performance. Firstly, the flexural yield of TRF members, connection method, and the number of VPGs has been studied [1]-[3]. This lateral resistant system was also checked by performing Endurance Time method (ET) which confirms the suitable flexural yield of TRF's members with different span lengths and alternate heights [4]. More ductility and better performance was obtained due to initial shear yielding specially in HPGs caused by decreasing their length [5]. The initial experimental and numerical studies on TRF against shear and flexural yield of H.P.Gs were investigated [6] and the experimental and numerical studies on 1:2 scale TRF were developed to show the adequate behavior and more ductility factor of TRF with shear yield of HPGs [7]. According to related literature and basis assumption of seismic design, HPGs are approximated to link beam in EBF, and VPG performs as a stiffened shear wall without elastic buckling [6]. Section properties of the VPG and HPGs have a major effect on the ductility and energy dissipation of the TRF systems. In this paper, actual behavior and ductility factor are assessed in TRF specimen. Shear and flexural yielding in HPGs is studied by four finite element models which verify the numerical results from the test and also developing the numerical studies.

Helia Barzegar Sedigh, Msc. Grad., is with the Department of Civil Engineering, Imam Khomeini International University, Qazvin, 34149-16818, Iran (corresponding author, e-mail: helia.barzegarsediq@yahoo.com).

Farzaneh Hamedi, Assistant professor, is with the Department of Civil Engineering, Imam Khomeini International University, Qazvin, 34149-16818, Iran.

Payam Ashtari, Assistant professor, is with the Department of Civil Engineering, University of Zanjan, Zanjan, 45371-38791, Iran.

II. Introducing TRF

TRF system is an I-shaped plate girder which is vertically placed at the middle of span (VPG), connected with two other HPGs to the side columns at each story level by the use of rigid connections (Fig. 1). TRF is introduced to have a shear or flexural yielding of HPGs and secondly, the yield of VPG. Assumptions of fixed or simple base joint of side columns are compared to provide appropriate seismic characteristics. This will fulfill architectural considerations such as locating openings.

Load distribution in T members would result in better performance of system by controlling the axial force of side columns and also by creating more resisting moment in base due to VPG [3]. Novelty of TRF needs more attention to design parameters such as width to thickness ratio. As it is possible for VGP's web to be compact or even non-compact, the stability and stiffness can be provided by web stiffeners. In comparison to EBF system, compression force and shear buckling of web in plastic zone are controlled with an optimal design by applying simple base joint in TRF side columns. In addition, flange compaction and appropriate placing of horizontal web stiffeners in VPG are precluded the global and local elastic buckling. In this case, stable and growing hysteresis curve without loss of lateral resistance and stiffness, are derived. It can be inferred that TRF with yield of three ductile members and lateral stability presents better seismic lateral behavior.

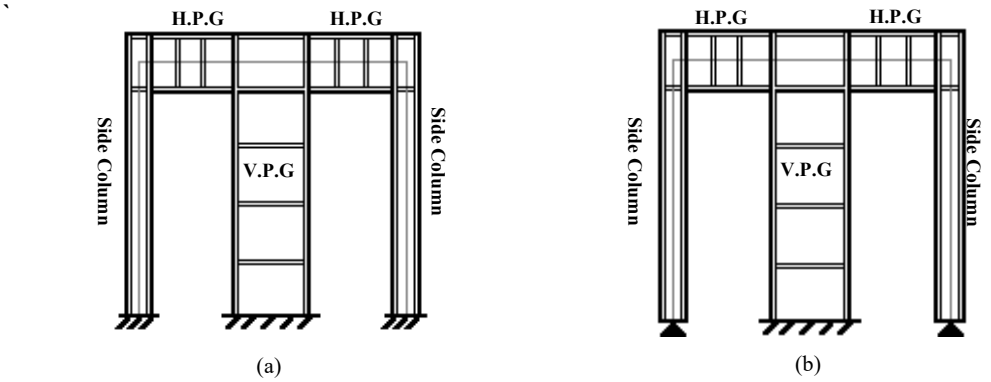

(a) (b)

Fig. 1 Configurations of TRF with side columns: (a) fixed and (b) simple base joint

III. Seismic Parameters

A. Design of Transverse Stiffeners

Web stiffeners of HPGs are designed for increasing stiffness to control local buckling. Primary distance (a) assumption is used as EBF's link beam with values given by AISC341-10 (2010) [8].

VPG's web stiffeners are designed in order to maintain general and local stability with respect to the fact that VPG as a ductile member of TRF is not designed to resist plastic shear capacity of HPGs. Here, the distance of web stiffeners is proposed as an average of upper limit of stiffeners' distance of HPGs and transverse stiffeners distance which are used to develop the available web shear strength (shown by a_{oi}). This proportion is expressed by (1).

$$a = \frac{(50 \cdot t_W - \frac{d}{5}) + a_{oi}}{2} \quad (1)$$

B. Loading Protocol

For estimation of system's behavior, cyclic loading protocol can be used [9]. Moment frame's cyclic load protocol is chosen according to AISC-Seismic Provision2010 (Fig. 2).

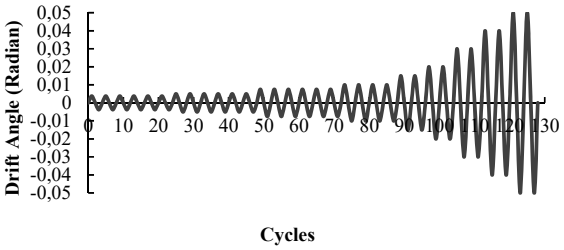

Fig. 2 Cyclic load protocol [8]

IV. Modeling

A. Details of Modeling and Design

A 1:2 scale sub-assembly of top floor of a five-story building is fabricated for experimental study. Surveys are done over half scale 3D, rectangular, and symmetric structure, according to former studies [6] with 1.5 m story height, by applying Special Concentrically Braced Frames (SCBFs) in the one direction and TRF in three spans located at sides and middle of the other direction. Span length of TRF is selected equal to certain length which may lead to shear yield of HPGs, equal to $\frac{1}{5}$ of span in former studies (equal to 0.55 m).

For developing the numerical study 4 full scale frames are derived from 3D, rectangular, and symmetric structure, according to former studies [6] with 3 m story height and 1.645 m HPGs length for the first and second floor, 1.695 m for the third and fourth floor, and 1.745 m for fifth floor. Static analyses parameters are applied according to ASCE-7-10 [10] shown in Table I.

TABLE I
Linear Static Analysis Parameters

Type of soil: D, Seismic Design Category: D	
T_O=0.15 s	T_O=0.15 s
I=1, ρ=1, K=1, Ω=2	
R_{WY}=8	R_{WX}=6
T_Y=0.0731(H)$^{3/4}$	T_X= (H)$^{3/4}$
C_d=5	C_d=4

TABLE II
Introduction of Models

MODELS#	ABBREVIATION of MODELS
1	finite element simulation of the TRF specimen with gravity load
2	Test
3	Verification of the test by finite element simulation
4	5 story TRF's frame with shear yield of H.P.Gs and rigid base joints of side columns
5	5 story TRF's frame with flexural yield of H.P.Gs and rigid base joints of side columns
6	5 story TRF's frame with shear yield of H.P.Gs and simple base joints of side columns
7	5 story TRF's frame with flexural yield of H.P.Gs and simple base joints of side columns

HPGs are designed based on EBF's link beam and VPG's standards based on plastic shear capacity of stiff shear walls and plastic moment capacity of SMRF's columns according to AISC-Seismic Provision 2010 [8]. Side columns are designed as component of a special moment resisting frame. Proportion of width to thickness is considered as highly ductile members. Members and web stiffeners of models which are introduced

in Table II are presented in Tables III and IV, respectively. The thickness of continuity plates in all side columns is calculated as 3 cm. Dimensions of HPGs of the frames with same span length are chosen to have a shear yielding or flexural yielding considering shear yield condition of $e \prec \frac{1.6M_P}{V_P}$ and flexural yield condition of $e \succ \frac{2.6M_P}{V_P}$, simultaneously ($M_P$: Plastic Moment strength, V_P: Plastic Shear strength).

TABLE III
GEOMETRIC PROPERTIES OF TRF MEMBERS

MODELS#:1-3			
Side Columns IPB100		V.P.G (cm) t_f= 1, b_f=10, t_w=0.4, h_w =26	H.P.Gs (cm) t_f= 1, b_f=7, t_w=0.3, h_w =13
MODELS#:4 and 6			
1st and 2nd Floor	Side Columns 45x45x2.5	V.P.G (cm) t_f= 2.5, b_f=30, t_w=0.8, h_w =71	H.P.Gs (cm) t_f= 2, b_f=25, t_w=0.8, h_w =45
3rd Floor	Side Columns 35x35x2	V.P.G (cm) t_f= 2.5, b_f=30, t_w=0.8, h_w =71	H.P.Gs (cm) t_f= 2, b_f=25, t_w=0.8, h_w =45
4th Floor	Side Columns 35x35x2	V.P.G (cm) t_f= 2.5, b_f=30, t_w=0.8, h_w =71	H.P.Gs (cm) t_f= 1.5, b_f=20, t_w=0.6, h_w =35
5th Floor	Side Columns 25x25x1.5	V.P.G (cm) t_f= 2.5, b_f=30, t_w=0.8, h_w =71	H.P.Gs (cm) t_f= 1.5, b_f=20, t_w=0.6, h_w =35
MODELS#:5 and 7			
1st and 2nd Floor	Side Columns 45x45x2.5	V.P.G (cm) t_f= 2.5, b_f=30, t_w=0.8, h_w =71	H.P.Gs (cm) t_f= 2, b_f=20, t_w=2, h_w =38
3rd Floor	Side Columns 35x35x2	V.P.G (cm) t_f= 2.5, b_f=30, t_w=0.8, h_w =71	H.P.Gs (cm) t_f= 2, b_f=20, t_w=2, h_w =38
4th Floor	Side Columns 35x35x2	V.P.G (cm) t_f= 2.5, b_f=30, t_w=0.8, h_w =71	H.P.Gs (cm) t_f= 1.5, b_f=20, t_w=1.5, h_w =28
5th Floor	Side Columns 25x25x2	V.P.G (cm) t_f= 2.5, b_f=30, t_w=0.8, h_w =71	H.P.Gs (cm) t_f= 1.5, b_f=20, t_w=1.5, h_w =28

t_f: flange thickness, b_f: flange width, t_w: web thickness, h_w: web height.

TABLE IV
CLEAR DISTANCE AND DIMENSIONS OF WEB STIFFENERS

MODELS#		V.P.G (cm)	H.P.Gs (cm)
1-3		t_s=1, h_s=24, b_s=4.5, a=30	t_s=1, h_s=13,b_s=3.3, a=12.3
4 and 6	1st-3rd Floor	t_s=1.5, h_s=71, b_s=14.6, a=51	t_s=0.8, h_s=45,b_s=12, a=31
	4th and 5th Floor		t_s=0.8, h_s=35,b_s=9.7, a=22
5 and 7	1st and 2rd Floor	t_s=1.5, h_s=71, b_s=14.6, a=51	t_s=0.4, h_s=38,b_s=9, a=89.5
	3rd Floor		t_s=0.4, h_s=38,b_s=9, a=94.5
	4th Floor		t_s=0.4, h_s=28,b_s=9, a=109.5
	5th Floor		t_s=0.4, h_s=28,b_s=9, a=114.5

t_s: stiffeners thickness, h_s: stiffeners height, b_s: stiffeners width, a: clear distance of web stiffeners.

B. Test Setup

50 tons capacity static hydraulic jacks and load cells which are installed at two sides of frame as shown in Fig. 3 are used to apply and measure force. Linear Variable Displacement Transducers (LVDTs) are installed to measure lateral displacement, out of plane deformations and diagonal deformation and chord rotation caused by shear yielding and the rest of LVDTs control accuracy of experiment. Out of plane torsion and buckling is controlled by two adjacent IPE140 placed at the top of frame in Fig. 3 [11]. Moreover, 28 5 mm strain gauges of 120 Ω (2% strains, gauge factor 2.23) are installed on the frame. Strain gauges are installed on the most probable yield places to monitor specifically shear yielding along 45 degree angle on the webs of HPGs and VPG and other were installed on the webs and flanges of HPGs and VPG along axial axis. In order to observe the yield patterns and progression, steel specimens are whitewashed by lime in the test center.

C. Finite Element Models

Non-linear behavior in ABAQUS is studied by von Mises stress in accordance with yield stress [12]. Shell element (S4R) having a reduced integration scheme is assumed for meshing of the existing domain to study the response of the frame under transverse shear force. In verification finite element model, HPGs, angles and web stiffeners are merged together at mesh's knot points. VPG and side columns with continuity plates, web stiffeners etc. are merged at knot points of mesh. HPGs' flanges and bearing plates are only tied wherever their surfaces are close to each other in order to make the degrees of freedom equal in this pair of surfaces. Web angle's leg and vertical members' flanges are also tied together only where the surfaces are close to one another. Approximate size for each mesh of HPGs and their merged

parts are defined as 1x1 cm^2. Also, mesh size for side columns, VPG and other members are 2x2 cm^2. Static general analysis and non-linear kinematic hardening are used with consideration of non-linear geometry. Table V represents extracted material parameters suggested by standard experiment ASTM-E8-04. For developing numerical studies, non-linear behaviors of 4 full scale frames are studied in ABAQUS with Push-over method according to FEMA356 [13]. Members' boundary conditions for 1:2 and full scale models with rigid condition of side columns are defined as shown in Fig. 4. To make simple base joint for side columns, the amount of displacement boundary conditions of reference points that are introduced at the base of each side columns are defined as zero. In addition, for the beginning of push-over analysis according to FEMA356 [13] the gravity loads in each story are applied in ABAQUS by body load and pressure on the H.P.Gs flanges, and then lateral displacements (U_3) are applied in each story according to FEMA356 [13]. Also, the whole members in 4 full scale frames are merged together and approximate size for each mesh are defined 5x5 cm^2. Other details of these 4 models are the same as verification model. Effects of large deformations are considered.

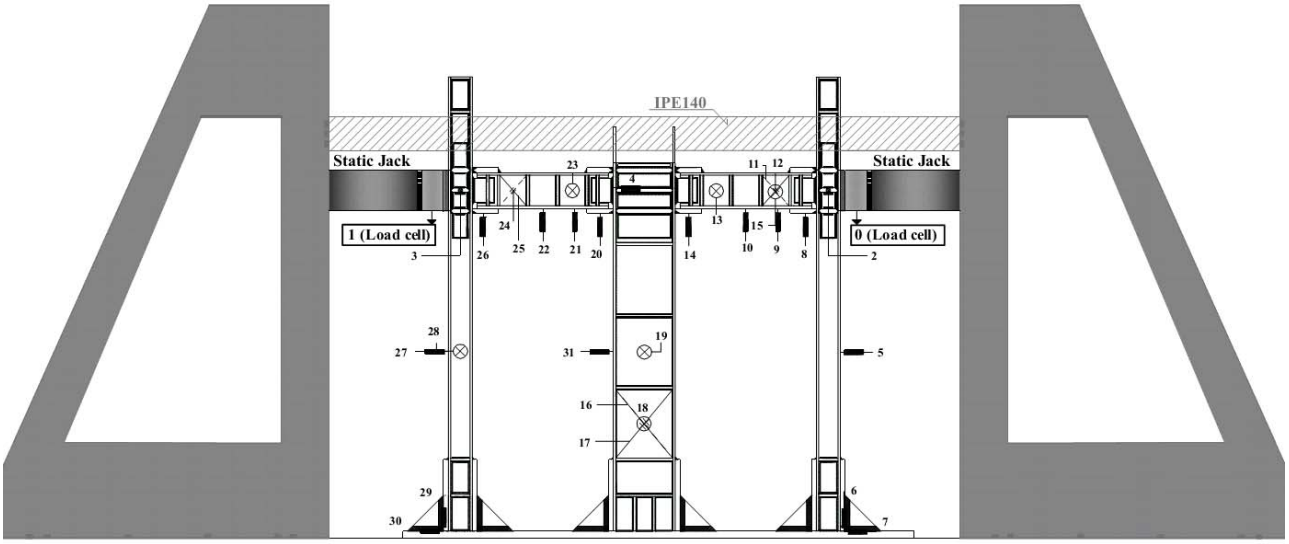

Fig. 3 Test setup: load cells and LVDTs

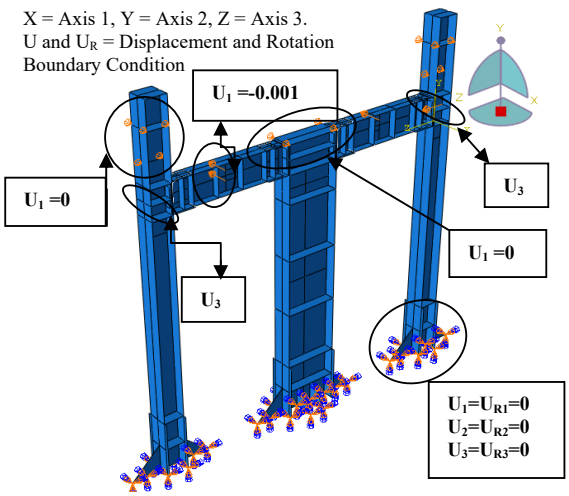

Fig. 4 Boundary conditions

V. Non-Linear Analyses

A. Experiment

According to the approximate equality (ultralow relative difference (2.7%)) in the values of forces and residual deformations of the test specimen under cyclic loading observed by numerical study (model 1), there was no need to apply any gravitational load for test.

TABLE V
Results of Tensile Test of Plates Used in the Experiment and Numerical Models

Plates Thickness (mm)	Yield stress F_y(kg/cm^2)	Ultimate stress F_u (kg/cm^2)	Ultimate strain ε_u	Plastic strain ε_P
3	2636.85	4609.15	0.236	0.234
4	2701.35	4360.51	0.256	0.254
6	2649	4745.44	0.22	0.216
10	2497	4461.3	0.25	0.246
20	2534.9	5127	0.177	0.174

At the cycle 6 of main protocol began, uniform yield in whole panels of HPGs, development of cracks in the whitewashed paint happened all over the webs. All these phenomena were proved by high values of strain recorded by diagonal strain gauges. At the end of cycle 17 and the beginning of cycle 18, system's non-linear behavior occurred right at lateral displacement of 7.6 mm, by development of HPGs' web diagonal tension field. In addition, at the end of cycle 17 because of the force redistribution, yield of VPG's web occurred. Phenomena such as formation of diagonal tension field, plastic chord rotation, local cracks in the whitewashed paint of HPGs' flanges and stiffeners, and

wrinkling, occurred during the experiment because of H.P.Gs' shear yielding. At the 30th cycle, next mechanism reached its critical limit as permanent deformations were increased. After this cycle, diagonal deformation of HPGs' web was the main phenomena that determine capacity of system (Fig. 5 (a)). Axial strain gauges located at H.P.Gs' web indicated that no axial force was being applied. There was also a diagonal tension field formed in V.P.G's panels right at cycle 30, especially near base joint (Fig. 5 (b)).

At the beginning of 33rd cycle, load was transferred to the VPG as a stiffened member, as a result of wrinkling at the HPGs' web without any significant loss of resistance. In addition, shear yielding and formation of plastic hinges resulted in a loss of capacity. Maximum lateral displacement was 51.15 mm at 33rd cycle (Fig. 6). As it is shown in Fig. 6, yield has been occurred in the whole length of HPGs' and VPG's webs because of appearing cracks in the whitewashed paint. Therefore, shear yielding of ductile members of TRF before side columns is proved. Such large deformations and resultant failure indicates that the test's end point should be considered at the previous cycle (33rd cycle). Yielding mechanism sequence for evaluation of TRF was: 1. Uniform shear yielding in HPGs' web; 2. Out of plane deformation as wrinkling and diagonal tension field formation in H.P.Gs' web; 3. Local yield of H.P.Gs' flanges around the web stiffeners by formation of diagonal tension field (Fig. 5 (a)); 4. Shear yielding and then formation of diagonal tension field in V.P.G's web. Hysteresis curve of experimental model is illustrated in Fig. 7.

Fig. 7 shows a stable hysteretic behavior with adequate energy dissipation caused by plastic deformation without any loss of lateral resistance and stiffness up to capacity limit. Gradual degradation of resistance and deterioration of stiffness is one of the advantages of TRF.

(a) (b)

Fig. 5 Uniform shear yielding and diagonal tension field (30th cycle) formation in web of: (a) H.P.G, (b) V.P.G

Fig. 6 TRF frame deformations at the last cycle of experiment (33rd)

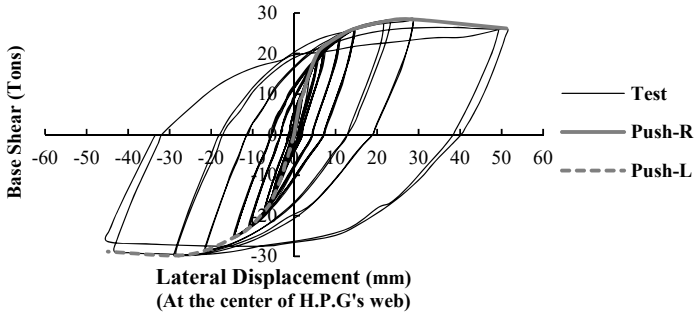

Fig. 7 Hysteresis curve of model 2 (experiment) and its push curves in each cycle

B. Finite Element Analyses

1) Verification and Seismic Characteristics

Verification of the developed numerical studies by finite element simulation is carried out by analyzing the shear yielding through presentation of von Mises stresses tension.

In Fig. 8 according to von Mises stresses, web diagonal yield due to diagonal tension field action and wrinkling phenomena are illustrated. Also, the members' web does not have any sign of elastic buckling; therefore, stability design is approved. Hysteresis curve and seismic characteristics are illustrated in Fig. 9 and Table VI (V_y, V_{max}: Yield and Maximum Base Shear and K_e: Effective stiffness, corresponding to slope of first line of bilinear capacity diagram, elastic stiffness) which approve system's high ductility in addition to sufficient lateral stiffness. In addition, residual deformations with relative difference of 12.5%, between experiment and finite element model prove the accuracy of simulation. Energy dissipation by plastic shear deformation in all loading cycles is obtained $1.76x10^6$ Kg.cm by finite element model and $1.46x10^6$ Kg.cm by experiment which are the area of hysteresis loops in Fig. 9. Thus, verification with relative difference of 17.1% is proved. Comparison between TRF and passive control by vertical link beam in EBF system proves that TRF has better lateral behavior because of yield in three ductile members and lateral stability derived from members' shear stiffness. In the experiment, TRF had ductility factor of 6.7 and lateral stiffness of 2916.8 kg/mm. Therefore, TRF presents higher ductility and stiffness in comparison to EBF with vertical link beam having corresponding amounts of 4.3 and 2734.5 kg/mm [14].

2) Numerical Studies

In model 4, 5 story TRF's frame with shear yield of HPGs and rigid base joints of side columns and in model 5, 5 story TRF's frame with flexural yield of HPGs and rigid base joints of side columns are simulated. Von Mises stresses of model 4 illustrates that chord rotation of HPGs caused by shear yield in whole HPGs' web in all stories and then shear yield of VPG's web in first and third floor result in a reduction of strength capacity and ductile behavior of TRF (Fig. 10 (a)). Also, redistribution of force to the side columns causes plastic hinges formation in base. Fig. 10 (b) shows von Mises stresses in model 5; high strength capacity and less ductile behavior in comparison to model 4 is proved by flexural yield of H.P.Gs' then widespread shear yielding of V.P.G's web panels. Redistribution of force to the side columns causes plastic hinge formation in base. In model 6, with shear yield of HPGs and simple base joints of side columns and in model 7, with flexural yield of HPGs and simple base joints of side columns are simulated. Von Mises stresses of model 5 illustrates that chord rotation of HPGs caused by shear yield in whole HPGs' web in all stories and then shear yield of VPG's web in first and third floor result in a reduction of strength capacity and ductile behavior of TRF (Fig. 11 (a)). In comparison to model 4, the reduction of strength capacity and ductility factor due to simple base joint of side columns is shown in Table VII. Fig. 11 (b) shows von Mises stresses in model 7, high strength capacity and less ductile behavior in comparison to model 6 is proved by flexural yield of HPGs' flanges near side columns and VPG and then widespread shear yielding of VPG's web panels as a TRF's stiff member in most stories. In comparison to model 5, the reduction of strength capacity and ductility factor due to simple base joint of side columns is shown in Table VII.

TABLE VI
SEISMIC CHARACTERISTICS OF TRF SPECIMEN AND ITS FINITE ELEMENT MODEL

MODELS#	Δ_y(mm)	Δ_{max}(mm)	μ	
2	7.6	51.15	6.73	
3	6.98	51.17	7.33	
Relative Difference (%)	8.2	-	8.18	
MODELS#	V_y(kg)	K_e^* (Kg/mm)	V_{max}(kg)	
2	22168	2916.84	-29801	28560
3	23294.9	3337.51	-25729	26408.2
Relative Difference (%)	4.8	12.6	11.36	7.5

Seismic characteristics of the models are indicated in Table VII. In the model 4 by shear yield of HPGs' web, then shear yield of VPG's web and formation of plastic hinge in side columns near base, lateral resistance decrease due to reduction of plastic shear capacity of VPG whereas, ductility factor increases because of HPG's chord rotation in comparison to model 5. In the model 6, appropriate lateral stiffness with decrease of base shear capacity are assessed because of its simple base joint of side columns and the same ductility in comparison to model 4. According to Table VII, in the models 5 and 7 by flexural yield of HPGs (link beams) and

widespread shear yield in VPG's web as a stiff member of TRF system, least ductility factor and most shear capacity without any significant rising of lateral stiffness are achieved. Highest ductility factor as it is shown in Table VII belongs to models 3, 4 and 6 which have shear yield of HPGs' web. Small percentages of strain hardening in Table VII, is achieved in these models, due to its ductile behavior.

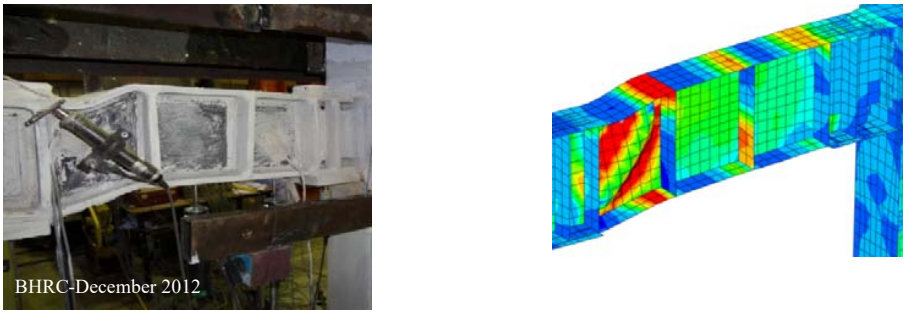

(a) (b)

Fig. 8 Yield and deformation of H.P.G in: (a) TRF specimen, (b) finite element model

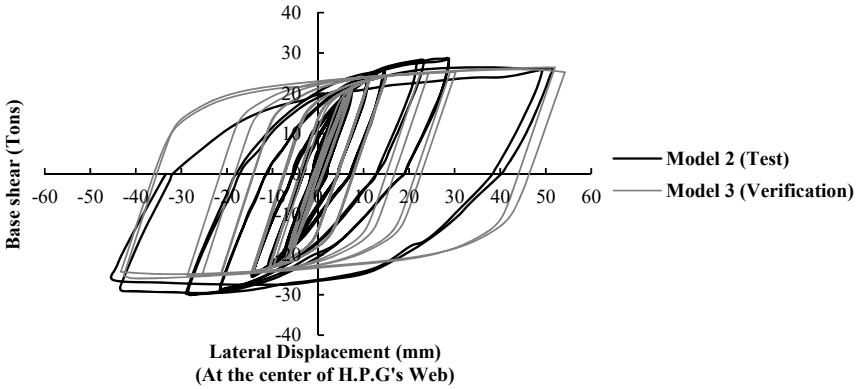

Fig. 9 Verification of hysteresis curves of model 2 and model 3

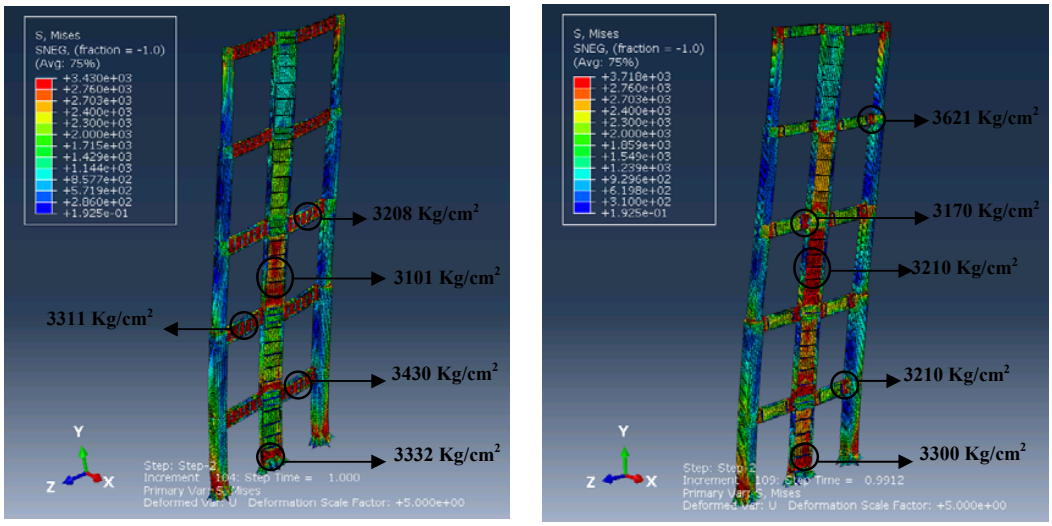

(a) (b)

Fig. 10 von Mises stresses in (a) model 4, (b) model 5

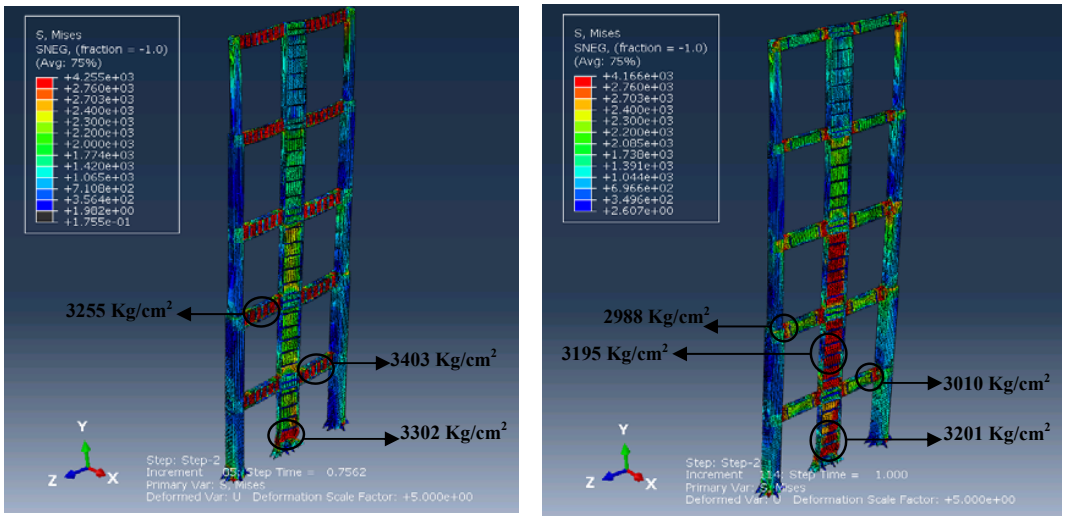

(a) (b)

Fig. 11 von Mises stresses in (a) model 6, (b) model 7

TABLE VII
SEISMIC CHARACTERISTICS OF MODELS 2-7

MODELS#	Δ_y(mm)	Δ_{max}(mm)	μ
2	7.6	51.15	6.73
3	6.98	51.17	7.33
4	83.49	556.151	6.66
5	101.43	473.99	3.76
6	77.62	476.83	6.14
7	91.86	305.86	3.33

MODELS#	V_y(kg)	K_e(Kg/mm)	V_{max}(kg)	Strain hardening (%)
2	22168	2916.84	28560	-
3	23294.9	3337.51	26408.2	2.11
4	156456.1	187384.4	179394	2.59
5	186702.1	184070.4	216005	5.68
6	133128.7	171520.4	151823	2.73
7	157913.6	171904.2	183594	6.98

VI. CONCLUSIONS

TRF is a ductile and lateral resistant system considering shear yielding of its H.P.Gs and V.P.G based on experimental and numerical studies. Following are primary conclusions achieved:

1. Ductility factor of TRF with shear yielding of link beams (H.P.Gs) is estimated 6.7 with lateral stiffness of 2916.8 kg/mm from experiment and these parameters are evaluated by finite element models as 7.3 and 2146.5 kg/mm for its finite element model having simple base joint of side columns. This illustrates that TRF has high ductility in addition to the large lateral stiffness simultaneously.
2. Stable, progressive and voluminous hysteresis curve without any significant lateral resistance degradation and deterioration of stiffness (up to capacity limit) is assessed.
3. Rigid connections of side column base joint with shear yield of its H.P.Gs will make a ductile behavior with appropriate lateral stiffness and shear capacity of TRF system.
4. TRF with simple base joint of side columns and its V.P.G behaves like a ductile lateral resistant system with more lateral stiffness compared to eccentrically braced frame without axial force in its link beams. Additionally, presence of two link beams (H.P.Gs) in spite of one in EBF results in higher degrees of indeterminacy in comparison to EBF.
5. Width to thickness ratio is better to be like high ductile members.

REFERENCES

[1] Ashtari, P. and Bandehzadeh, M. (2009), "Seismic Evaluation of New Crucial Beam-Column Lateral Resistant System", *8th National Congress on Civil Engineering*, Shiraz University, Shiraz, Iran.
[2] Ashtari, P. and Abbasi, A.A. (2010), "Evaluation of Response Modification Factor of Different Shape of TBR", *International Conference on Seismology*, Kerman University, Kerman, Iran.
[3] Bandehzadeh, M. and Ashtari, P. (2014), "T-Resisting Frame Concept: Headway towards Seismic Performance Improvement of Steel Frames", *J of Constructional Steel Research*, **104**, 193-205.
[4] Gorzin, M. (2011), "Seismic Assessment of TBF Resistant Frame With Endurance Time Method", Thesis for the degree of Master of Science, Civil Engineering Department, Faculty of Engineering, Zanjan University, Zanjan , Iran.
[5] Ashtari, P., Hamedi, F., Barzegar Sedigh, H., and Rasouli, I, (2012), "Comparison of Seismic Responses of T Resistant Frame (TRF) with Shear or Bending Yielding in Link Beams", *15th World Conference on Earthquake Engineering*, Lisbon, Portugal.
[6] Barzegar Sedigh, H. (2013), "Investigation of Seismic Behavior of T Resistant Frame (TRF) with Link Beams Having Shear or Moment Yielding", Thesis for the degree of Master of Science, Department of Civil Engineering, Faculty of Engineering and Technology, Imam Khomeini International University, Qazvin, Iran.
[7] Ashtari, P., Barzegar Sedigh, H., Hamedi, F. (2016), "Experimental and Numerical Study on Innovative Seismic T-Resisting Frame (TRF)", *J of Structural Engineering and Mechanics*, **60**(2), 251-269.
[8] AISC341-10, (2010), Seismic Provisions for Structural Steel Buildings, ANSI-AISC 341-10, Chicago, IL: American Institute of Steel Construction.
[9] Krawinkler, H. (2009), "Loading History for Cyclic Testing in Support of Performance Assessment of Structural Component", Department of civil and Environment Engineering, Stanford University, Stanford,

California, USA.
[10] ASCE/SEI 7-10, (2010), Seismic rehabilitation of existing buildings. s. l, IL: American Society of Civil Engineers.
[11] Farshchi, H., Moghadam, A.S., and Jazany, R.A. (2011), "Experimental and Analytical Study of Connection Strength Effect in X-Type Braced Frames", *Modares J Civil Engineering*; **11**(4), 69-134.
[12] Bahrampoor, H. and Sabouri Ghomi, S. (2010), "Affect of Easy-Going Steel Concept on the Behavior of Diagonal Eccentrically Braced Frames", *J of Civil Engineering*, **8**(3), 242-255.
[13] FEMA 356, (2000) Federal Emergency Management Agency. Washington DC, IL: NEHRP Guidelines for the Seismic Rehabilitation of Buildings. Report No 356.
[14] Zahrae, S.M. (2009), *Behavior of Vertical Link Beam in Steel Building*, BHRC Publish No. R-515, Tehran, Iran.